

Characterization of boron-doped diamond electrodes by electrochemical impedance spectroscopy

K. JÜTTNER* and D. BECKER

DECHEMA e.V., Karl-Winnacker-Institute, Theodor-Heuss-Allee 25, D-60486 Frankfurt am Main, Germany

(*author for correspondence, e-mail: juettner@dechema.de)

Received 14 February 2006; accepted in revised form 8 April 2006

Key words: boron doped diamond, electrochemical impedance spectroscopy, partially blocked electrode

Abstract

Charge transfer on boron doped diamond (BDD) electrodes was studied by cyclic voltammetry and electrochemical impedance spectroscopy. The diamond films of 5 μm thickness and boron content between 200 ppm and 3000 ppm were prepared by the hot filament CVD technique on niobium substrate and mounted in a Teflon holder as rotating disk electrodes. The electrochemical measurements were carried out in aqueous electrolyte solutions of 0.5 M $\text{Na}_2\text{SO}_4 + 5 \text{ mM K}_3[\text{Fe}(\text{CN})_6]/\text{K}_4[\text{Fe}(\text{CN})_6]$. Significant deviation in the redox behaviour of BDD and active Pt electrodes was indicated by a shift of the peak potentials in the cyclic voltammograms with increasing sweep rate and lower limiting diffusion current densities under rotating disk conditions. In the impedance spectra an additional capacitive element appeared at high frequencies. The potential and rotation dependence of the impedance spectra can be described quantitatively in terms of a model based on diffusion controlled charge transfer on partially blocked electrode surfaces. Direct evidence for the non-homogeneous current distribution on the diamond surface was obtained by SECM measurements.

1. Introduction

Boron-doped diamond has attracted much attention as electrode material due to its inherent electronic properties, chemical inertness and mechanical stability. In particular the wide potential window of up to 4 V in aqueous solutions makes this material attractive for technical applications in electrosynthesis and electro-analysis [1–8]. However, charge transfer between the diamond surface and redox species in solution is not yet fully understood and deserves closer consideration. Apparent rate constants of quasi-reversible “outer sphere” redox couples, such as $\text{Fe}(\text{CN})_6^{3-/4-}$, $\text{Ru}(\text{NH}_3)_6^{3+/2+}$, $\text{IrCl}_6^{2-/3-}$, $\text{Fe}^{2+/3+}$ were extracted from cyclic voltammograms and found to be several orders of magnitude lower than on carbon or platinum electrodes. This unusual behaviour was explained by electronic factors of the bulk material, surface states and impurity states in the band gap, the ohmic resistance of the film, or changes in the redox reaction mechanism [9–19]. However, as demonstrated in previous studies, the observed deviations can also be accounted for by partial blocking of the diamond surface [20–23]. A detailed discussion can be found in the paper of Bard et al. [23]. These authors have shown by simulation of cyclic voltammograms that neither uncompensated ohmic resistance nor changes in the apparent rate constants

can satisfactorily explain the observed behaviour of reversible diffusion controlled reactions. Direct evidence for the existence of active and inactive sites at the diamond surface depending on the dopant concentration was obtained from conductivity AFM and SECM measurements [23].

2. Experimental

Polycrystalline diamond films of 5 μm thickness with boron contents between 200 and 3000 ppm were prepared by the hot filament CVD technique on niobium substrate (FhG-IST Braunschweig [1]). Rotating disk electrodes (RDE) of 0.5 cm^2 geometrical area were prepared by embedding the samples in a Teflon holder. Measurements were carried out in a three-electrode cell at $T = 298 \text{ K}$ under defined convection and compared with Pt electrodes under the same conditions. An Ag/AgCl(sat. KCl) electrode with a Luggin capillary served as the reference and a platinum sheet of 2 cm^2 geometrical area as the counter-electrode. Aqueous solutions of 0.5 M $\text{Na}_2\text{SO}_4 + 5 \text{ mM K}_3[\text{Fe}(\text{CN})_6]/\text{K}_4[\text{Fe}(\text{CN})_6]$ were prepared from “p.a.” grade chemicals (Riedel-deHaen) and prior to the experiments purged with N_2 . Cyclic voltammograms at different sweep rates and electrochemical impedance spectra in the frequency range

$100 \text{ mHz} \leq f \leq 100 \text{ kHz}$ with 5 mV ac-amplitude were measured using Zahner IM5d equipment. The working electrodes were cleaned in an ultrasonic bath and activated by electrochemical cycling between oxygen and hydrogen evolution before starting the experiments. The SECM measurements were carried out with the newly developed ProScan instrument from HEKA Elektronik.

3. Results and discussion

Figure 1. shows cyclic voltammograms of $\text{K}_3[\text{Fe}(\text{CN})_6]/\text{K}_4[\text{Fe}(\text{CN})_6]$ on Pt and BDD electrodes at different sweep rates. The voltammograms on Pt exhibit the ideal behaviour of a reversible redox reaction with peak potential difference of about $\Delta E_p = 60 \text{ mV}$, which on BDD is larger and increases with increasing sweep rate v while the peak current densities decrease. Figures 2(a and b) show polarisation curves of $\text{Fe}(\text{CN})_6^{3-}/4^-$ on Pt and BDD for different rotation frequencies f_{rot} of the disk electrodes. On Pt the behaviour corresponds to that of an ideal diffusion controlled, reversible reaction, whereas on BDD the polarisation curves exhibit significantly larger overvoltages and a decrease in the limiting diffusion current density by approximately 20% is seen.

Figure 3. shows the impedance spectra in a Nyquist plot presentation for different rotation frequencies. On Pt the spectra exhibit the ideal shape of a purely transport controlled reaction which is described by the well known Nernst impedance:

$$Z_N(j\omega) = R_N \frac{\tanh \sqrt{j\omega/\omega_N}}{\sqrt{j\omega/\omega_N}} \quad (1)$$

where

$$R_N = \frac{2RT\delta_N}{z^2F^2c^sD}$$

and

$$\omega_N = \frac{D}{\delta_N^2}$$

with δ_N : thickness of the diffusion layer, c^s : steady state concentration at the electrode surface, and D : diffusion coefficient of reacting species. The parameters z , F , R and T have their usual meaning. For rotating disk electrodes $\delta_N \sim f_{\text{rot}}^{-1/2}$ as described by the Levich equation. At $f_{\text{rot}} = 0$ the thickness of the diffusion layer tends to infinity, $\delta_N \rightarrow \infty$, and Equation (1) turns into the expression of the Warburg impedance $Z_W(j\omega)$ for $\omega/\omega_N \gg 1$ (straight line in Figure 3(a)):

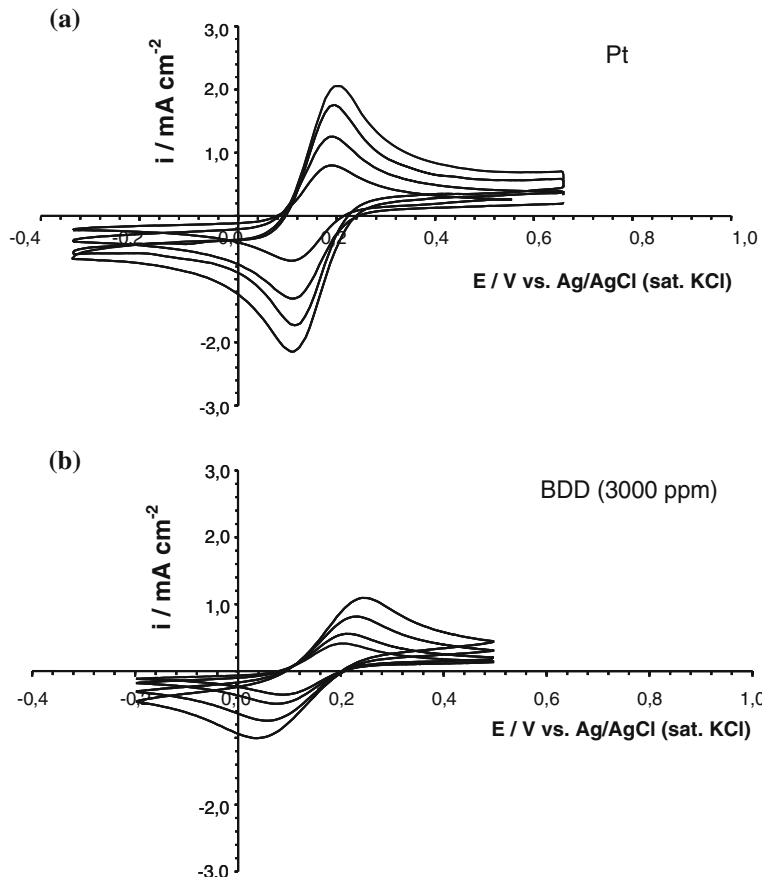


Fig. 1. Cyclic voltammograms of Pt (a) and BDD (b) in $0.5 \text{ M } \text{Na}_2\text{SO}_4 + 5 \times 10^{-3} \text{ M } \text{K}_3[\text{Fe}(\text{CN})_6]/\text{K}_4[\text{Fe}(\text{CN})_6]$; $|dE/dt| = 10, 20, 50, 100 \text{ mVs}^{-1}$; $f_{\text{rot}} = 0 \text{ rpm}$; $T = 298 \text{ K}$.

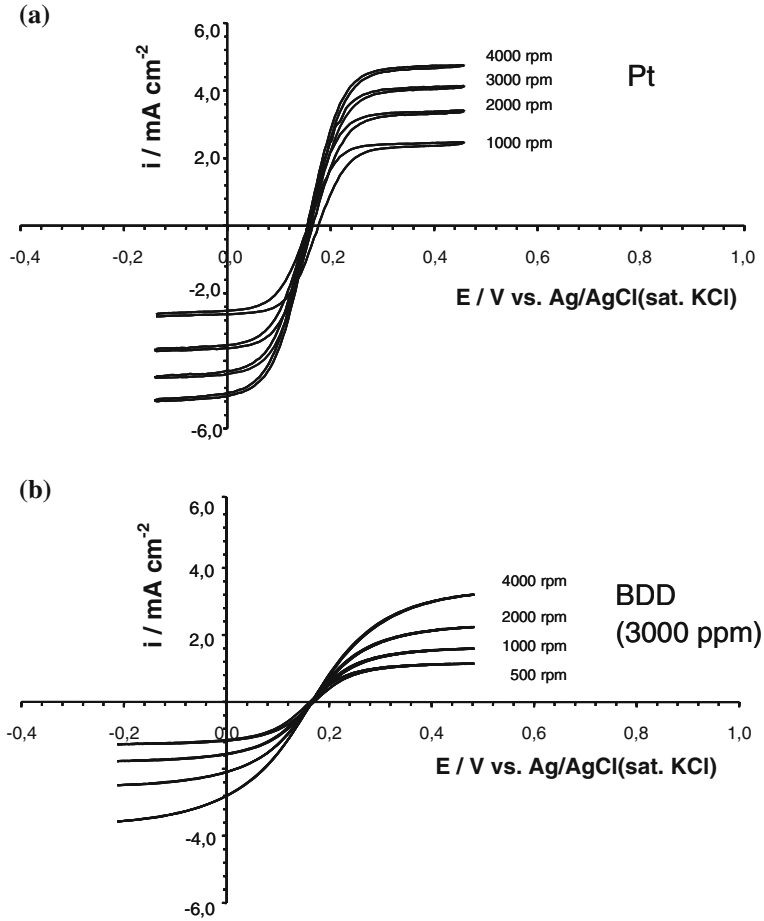


Fig. 2. Rotating disk polarisation curves of Pt (a) and BDD (b) in $0.5 \text{ M } \text{Na}_2\text{SO}_4 + 5 \times 10^{-3} \text{ M } \text{K}_3[\text{Fe}(\text{CN})_6]/\text{K}_4[\text{Fe}(\text{CN})_6]$; $500 \text{ rpm} \leq f_{\text{rot}} \leq 4000 \text{ rpm}$; $|\text{dE/dt}| = 100 \text{ mVs}^{-1}$; $T = 298 \text{ K}$.

$$Z_W(j\omega) = \frac{2RT}{z^2 F^2 c^s \sqrt{D}} \times \frac{1}{\sqrt{j\omega}} \quad (2)$$

The impedance spectra of Pt are well described by Equations (1) and (2), which is evident from the full line curves representing the fit of the experimental data in Figure 3. The BDD impedance in Figure 3(b) differs significantly from that of Pt. In addition to the Nernst impedance part at low frequencies, a capacitive loop is prominent at high frequencies showing only weak rotation dependence.

The overvoltage dependence of the BDD impedance is shown in Figure 4. Due to the decrease in the surface concentration c_s with increasing overvoltage η , the resistance R_N and the magnitude of the Nernst impedance increases (cf. Equation (1)). It should be noted that the capacitive high frequency loop of the BDD impedance spectra also increases, which indicates that this element cannot be considered simply as charge transfer resistance.

From the literature it is known that surface treatment of BDD affects the “electrochemical activity” of the diamond surface [20, 21, 24, 25]. It was found that anodic polarisation and mechanical polishing with

carbon cloth or SiC paper leads to an activation of BDD electrodes. This reveals that the activity of these electrodes is a surface property. We further concluded that the observed deviations of BDD can be traced back to a partial blocking of the electrode surface [18]. Reversible charge transfer takes place at high reaction rate (k_o) but is restricted to a limited number of active sites.

A model approach to describe the influence of partial blocking on transport controlled reactions was first discussed by Matsuda et al. [26] and later adapted by Schmidt et al. [27, 28] to derive the transfer function for such systems. Figure 5 gives a simplified scheme of the electrode/solution interface with random distribution of active and inactive sites and non-homogeneous concentration gradients and fluxes. The analytical solution of this non-linear diffusion problem leads to the following expression for the transport impedance $Z_{\text{tr}}(j\omega)$:

$$Z_{\text{tr}}(j\omega) = Z_N(j\omega) + \sigma \cdot Z_\sigma(j\omega) \quad (3)$$

which can be separated into the ideal Nernst impedance $Z_N(j\omega)$ and the perturbation term $\sigma \cdot Z_\sigma(j\omega)$ containing all the deviations from the ideal linear diffusion regime [27, 28].

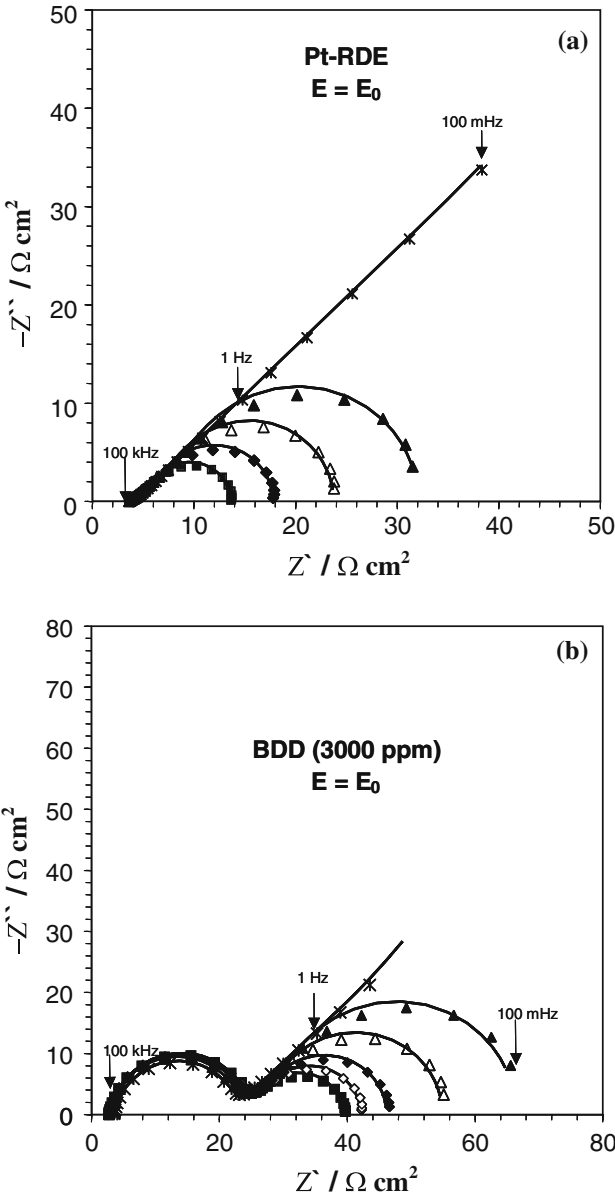


Fig. 3. Impedance spectra of Pt (a) and BDD (b) at equilibrium potential in $0.5 \text{ M Na}_2\text{SO}_4 + 5 \times 10^{-3} \text{ M K}_3[\text{Fe}(\text{CN})_6]/\text{K}_4[\text{Fe}(\text{CN})_6]$ at different rotation frequencies $f_{\text{rot}}/\text{rpm}$: 0 (*), 500 (▲), 1000 (△), 2000(◆), 3000(◇), 4000 (■); $T = 298 \text{ K}$.

$$Z_\sigma(j\omega) = R_\sigma \frac{\tanh \sqrt{(j\omega + W)/\omega_\sigma}}{\sqrt{(j\omega + W)/\omega_\sigma}} \quad (4)$$

where

$$R_\sigma = \frac{2RT\delta_\sigma}{z^2F^2c^sD}$$

and

$$\omega_\sigma = \frac{D}{\delta_\sigma^2}$$

The degree of surface blocking σ is expressed as ratio of the inactive and active surface area:

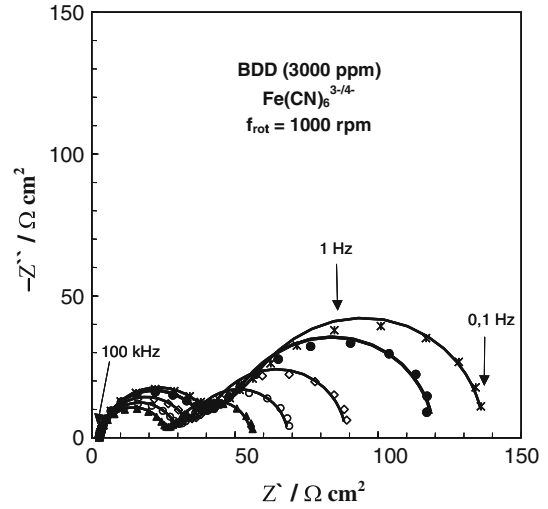


Fig. 4. Impedance spectra of BDD in $0.5 \text{ M Na}_2\text{SO}_4 + 5 \times 10^{-3} \text{ M K}_3[\text{Fe}(\text{CN})_6]/\text{K}_4[\text{Fe}(\text{CN})_6]$ at different overvoltage η/mV : 80 (*), 70 (●), 50(◇), 40 (○), 10 (▲); $f_{\text{rot}} = 1000 \text{ rpm}$; $T = 298 \text{ K}$.

$$\sigma = \frac{\pi R^{*2} - \pi a^2}{\pi a^2} \quad (5)$$

where a and R^* are the inner and outer radius of the circular patches of the respective active and inactive sites (Figure 5). The parameters R_σ , ω_σ and W depend on the thickness δ_σ of the non-homogeneous diffusion layer at the electrode surface with lateral concentration gradients and fluxes. The parameter W in Equation (4)

$$W = \frac{2D}{R^{*2}} \frac{(1 + \sigma)^2}{\sigma} \frac{1}{\ln(1 + 0.25\sqrt{1 + \sigma})} \quad (6)$$

can be considered as a characteristic frequency ($W \approx D/R^{*2}$) for lateral diffusion within the non-homogeneous transport layer.

The BDD impedance data were fitted by the model impedance $Z_{\text{tr}}(\omega)$ with a double layer capacitance C_{dl} in parallel. For Pt the double layer capacity was found to be $20 \mu\text{F cm}^{-2}$ whereas $7 \mu\text{F cm}^{-2}$ was found for BDD. There are five adjustable model parameters to fit the impedance data: R_N , ω_N , $\sigma \cdot R_\sigma$, ω_σ and W . As can be seen from the full line curves in Figures 3 and 4, the experimental impedance spectra are well described by the model. It should be noted that σ is not accessible directly but appears as factor in the product of the fitting parameter $\sigma \cdot R_\sigma$. For the separation of σ an approximate value of R_σ as calculated from R_N , ω_N and ω_σ according to:

$$R_\sigma = R_N \sqrt{\frac{\omega_N}{\omega_\sigma}} \quad (7)$$

A blocking factor $\sigma \approx 32$ was found independent of the rotation frequency. The parameters σ , R_σ and W , which are characteristic for partial blocking, are plotted in Figure 6 as a function of rotation frequency f_{rot} .

As expected, only weak dependence of W and σ on rotation frequency is found. The parameter R_σ decreases

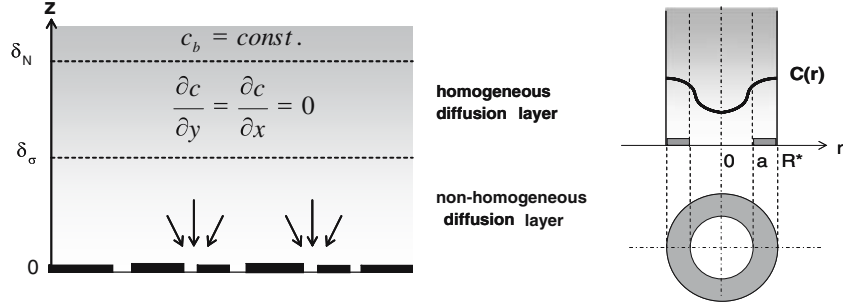


Fig. 5. Scheme of non-homogeneous transport layer at partially blocked electrode with active and inactive sites leading to lateral concentration gradients and fluxes [27].

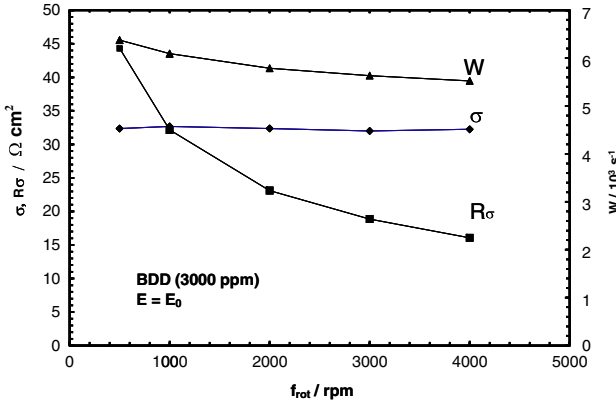


Fig. 6. Fit parameters R_σ , σ and W as a function of rotation frequency f_{rot} obtained from the fit of the experimental data in Figure 3(b).

with f_{rot} indicating that the thickness of the non-homogeneous diffusion layer, δ_σ , decreases proportional to the Nernst diffusion layer, δ_N . From σ and W the mean distance of active sites were estimated to be $R^* \approx 9 \mu\text{m}$, which is of the order of the diffusion layer thickness δ_N at $f_{\text{rot}} \approx 1000 \text{ rpm}$. It is well known that the influence of surface blocking on the limiting diffusion current density becomes significant if the distance of active sites is comparable or larger than the diffusion layer thickness [29]. This would also explain the lower values of the limiting diffusion current densities in Figure 2. The number of active sites $N^* (\approx 1/\pi R^{*2})$ was estimated to be $1 \times 10^6 \text{ cm}^{-2}$. The value for the mean distance of active sites, $2R^* \approx 18 \mu\text{m}$, is also in good agreement with SECM measurements. The SECM image in Figure 7 was obtained in feed back mode of

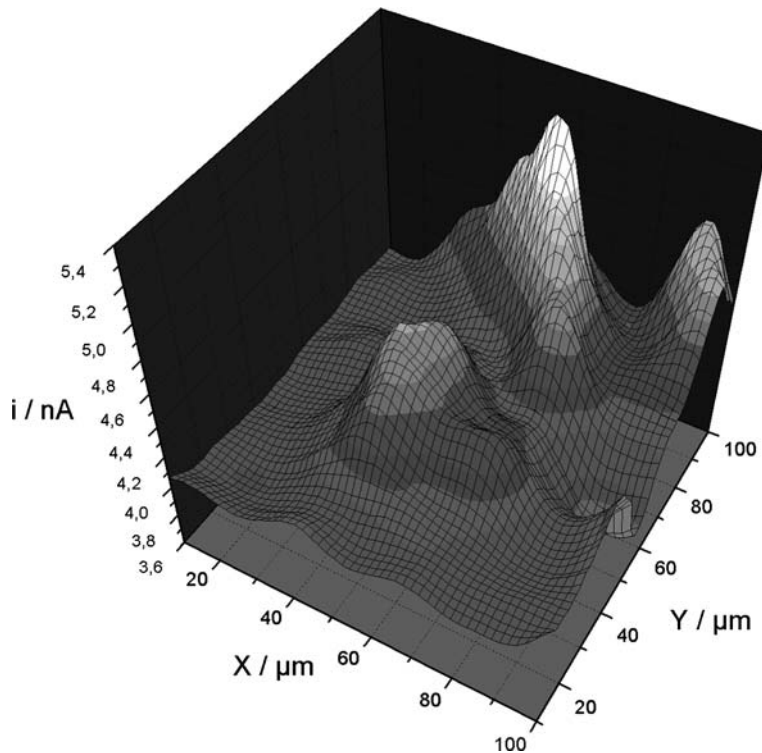


Fig. 7. SECM-image obtained at boron doped BDD(2000 ppm) in propylenecarbonate + 5 mm ferrocene + TBAPF₆ with Pt microelectrode (10 μm); scan rate 5 μm s⁻¹; tip distance 5 μm, potential 0.4 V; (ProScan, HEKA Elektronik).

a Pt microelectrode ($10\text{ }\mu\text{m}$) at $5\text{ }\mu\text{m s}^{-1}$ scan rate and constant tip distance with ferrocene as redox mediator in propylenecarbonate at 0.4 V . Hot spots on the diamond surface are indicated by the peaks in the feed back current profile.

4. Conclusions

It can be concluded that the low “electrochemical activity” of BDD electrodes can be interpreted in terms of partial blocking of the diamond electrode surface rather than by a change in rate constants of the “outer sphere” redox reactions. The partial blocking may be caused by a non-homogeneous distribution of the boron dopant in the diamond lattice, structural defects, non-diamond sp^2 carbon phases, segregation of carbon in grain boundaries and surface terminal groups.

Acknowledgements

The authors acknowledge financial support of this work by the Deutsche Forschungsgemeinschaft, DFG (JU 201–8). We also thank the Fraunhofer Institut für Schicht und Oberflächentechnik, IST Braunschweig, Germany, for providing the boron doped diamond films on niobium substrate. The authors are indebted to Dr. K. Bauer-Espindola, HEKA Elektronik, for the SECM measurements on BDD.

References

- I. Tröster, L. Schäfer and M. Fryda, *New Diam. Fron. Carbon Technol.* **12** (2002) 89.
- G.M. Swain and R. Ramesham, *Anal. Chem.* **65** (1993) 345.
- A. Fujishima, C. Terashima, K. Honda, B.V. Sarada and T.N. Rao, *New Diam. Fron. Carbon Technol.* **12** (2002) 73.
- P.A. Michaud, E. Mahe, W. Haenni, A. Perret and C. Comninellis, *Electrochem. Solid-State Lett.* **3** (2000) 7.
- W. Haenni, J. Gobet, A. Perret, L. Pupunat, P. Rychen, C. Comninellis and B. Correa, *New Diam. Fron. Carbon Technol.* **12** (2002) 83.
- H.J. Förster, W. Thiele, D. Fassler and K.G. Günther, *New Diam. Fron. Carbon Technol.* **12** (2002) 99.
- L. Gheradini, P.A. Michaud, M. Panizza and Ch. Comninellis, *J. Electrochem. Soc.* **148** (2001) D78.
- T. Yano, D.A. Tryk, K. Hashimoto and A. Fujishima, *J. Electrochem. Soc.* **145** (1998) 1870.
- S. Ferro and A. Battisti, *Electrochimica Acta* **47** (2002) 1641.
- I. Duo, C. Levy-Clement, A. Fujishima and Ch. Comninellis, *J. Appl. Electrochem.* **34** (2004) 935.
- I. Duo, A. Fujishima and Ch. Comninellis, *Electrochem. Commun.* **5** (2003) 695.
- F. Marken, C.A. Paddon and D. Asogan, *Electrochem. Commun.* **4** (2002) 62.
- J. van de Lagemaat, D. Vanmaekelbergh and J.J. Kelly, *J. Electroanal. Chem.* **475** (1999) 139.
- C.H. Goeting, F. Jones, J.S. Foord, J.C. Eklund, F. Marken, R.G. Compton, P.R. Chalker and C. Johnston, *J. Electroanal. Chem.* **442** (1998) 207.
- W. Schmickler, *Interfacial Electrochemistry* (Oxford University Press, 1996).
- Y.V. Pleskov, Y.E. Evstafeeva, M.D. Krotova and A.V. Laptev, *Electrochim. Acta* **44** (1999) 3361.
- M.C. Granger, M. Witek, J. Xu, J. Wang, M. Hupert, A. Hanks, M.D. Koppang, J.E. Butler, G. Lucazeau, M. Mermoux, J.W. Strojek and G.M. Swain, *Anal. Chem.* **72** (2000) 3793.
- G. Pastor-Moreno and D.J. Riley, *Electrochim. Commun.* **4** (2002) 218.
- K.B. Holt, G. Sabin, R. Compton, J.S. Foord and F. Marken, *Electroanalysis* **14** (2002) 797.
- D. Becker and K. Jüttner, *New Diam. Fron. Carbon Technol.* **13** (2003) 67.
- D. Becker and K. Jüttner, *J. Appl. Electrochem.* **33** (2003) 959.
- D. Becker and K. Jüttner, *Electrochim. Acta* **49** (2003) 29.
- K.B. Holt, A.J. Bard, Y. Show and G.M. Swain, *J. Phys. Chem.* **108** (B 2004) 15117.
- T.N. Rao, D.A. Tryk, K. Hashimoto and A. Fujishima, *J. Electrochem. Soc.* **146** (1999) 680.
- H.B. Suffredini, V.A. Pedrosa, L. Codognoto, S.A.S. Machado, R.C. Rocha-Filho and L.A. Avaca, *Electrochim. Acta* **49** (2004) 4021.
- T. Gueshi, K. Tokuda and H.J. Matsuda, *Electroanal. Chem.* **89** (1978) 247, **101** (1979) 29, **102** (1979) 41.
- J. Hitzig, J. Titz, K. Jüttner, W.J. Lorenz and E. Schmidt, *Electrochim. Acta* **29** (1984) 287.
- E. Schmidt, J. Hitzig, J. Titz, K. Jüttner and W.J. Lorenz, *Electrochim. Acta* **31** (1986) 1041.
- R. Landsberg and R. Thiele, *Electrochim. Acta* **11** (1966) 1243.